Prediction of Newtonian & Non-Newtonian Flow Through Concentric Annulus With Centerbody Rotation

J. A. Naser

CFD Consultant, CANCES-ATP, G16 National Innovation centre, ATP, Eveleigh 1430, Australia

Formerly, Associate Professor, Mechanical Engineering Department
Bangladesh University of Engineering & Technology, Dhaka-1000, Bangladesh

ABSTRACT

Numerical study is carried out for both laminar and turbulent flow through concentric annuli with centerbody rotation. Investigations are performed for two fluids, one Newtonian and the other a shear thinning non-Newtonian polymer. For turbulent flow, the governing equations are closed using the k-ε turbulence model. The equations are discretised using a finite volume technique. The central difference scheme is employed to evaluate the diffusion terms and a hybrid scheme is employed to evaluate the convection terms. Solutions are obtained using the SIMPLE algorithm. The results obtained, are compared with the existing experimental data. For laminar non-Newtonian flow, the velocities near the centerbody, show deviations from the experiment. These are attributed to the existence of turbulence due to the higher rotational speed of the centerbody. For turbulent Newtonian flow, good agreement is obtained for axial velocities, but tangential velocities show discrepancies. For turbulent non-Newtonian flow, both axial and tangential velocities show deviations. These are attributed to the deficiencies of the turbulence model used.

NOMENCLATURE:

K	non-Newtonian fluid consistency index
k	turbulent kinetic energy
n	power-law exponent
R_e	bulk flow Reynolds number $2\rho U(R_o-R_i)/\mu$
R_i	radius of inner-wall of annulus
R_o	radius of outer-wall of annulus
U	bulk axial velocity
u,v,w	axial, radial & tangential velocities
x,r,θ	coordinate directions
ε	turbulent kinetic energy dissipation
μ	characteristic fluid viscosity
μ_t	turbulent eddy-viscosity
ρ	fluid density
ξ	$x/(R_o-R_i)$
ζ	$(r-R_i)/(R_o-R_i)$

1. INTRODUCTION

Flows in annular passages with center body rotation are important in drilling wells. The drilling fluids, passing between the drilling shaft and the well casing, usually show non-Newtonian behavior. The previous theoretical and computational work is almost exclusively very concerned with laminar flow. Recent work includes that of Gucuyener and Mehmetoglu (1992), which considers analytical solution to the volumetric flow rate for pseudo plastic fluids in concentric annuli. The detail finite element study of Lockett et. al (1992) considers the general situation of combined axial and rotational motion. Computation of turbulent flow problems has received very little attention to date. However, turbulent flow for Newtonian fluid has been studied (e.g.. Sharma et al. (1976)).

Experimental works has recently received considerable attention. LDA measurements of flow velocities and turbulence intensities, for a shear thinning fluid, flowing through a concentric smooth walled annulus with a rotating centerbody, having radius ratio (R_o/R_i) of 0.506 has been performed by Escudier et al. (1995). The shear thinning fluid was prepared by adding 0.2% w/w of carboxymethylcellulose (CMC) to water.

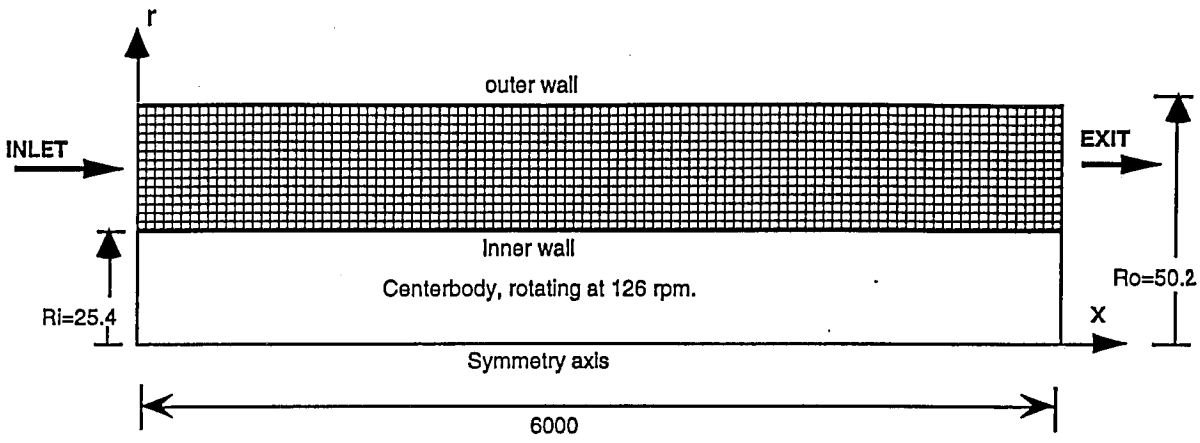

Fig. 1 Schematic representation of solution domain and computational grid (not to scale, dimensions in mm).

Other recent experimental works, directly relevant to the present study, are that of Nouri and Whitelaw (1994) and Naimi et al. (1990). The present study is a numerical simulation of the experimental work of Escudier et al. (1995). This work reports the computational study of developing fluid flow through concentric annuli with centerbody rotation. The study is carried out for both laminar and turbulent flow, using Newtonian and non-Newtonian fluids.

2. SOLUTION DOMAIN AND BOUNDARY CONDITIONS:

The solution domain used is the present study (Fig.1), is same as that of the experimental flow geometry used by Escudier et al. (1995). For Newtonian fluid, a mixture of glucose syrup and water (50% w/w) and for non-Newtonian fluid, a mixture of carboxymethylcellulose (CMC) and water (0.2% w/w) were used. The fluid properties and the value of fluid viscosity needed to calculate the Reynolds number for CMC were taken from Escudier et al. (1995). Predictions are performed under laminar flow assumptions, at R_e=800 & 350 for glucose and CMC respectively. Under turbulent flow assumptions, predictions are performed at R_e=7500 & 4400 for glucose and CMC respectively. Uniform values of flow variables were specified at the inlet. Zero gradient boundary conditions were employed at the exit. At the solid walls, no-slip boundary conditions were employed in conjunction with the log-law for turbulent cases.

3. THE GOVERNING EQUATIONS:

For incompressible non-Newtonian fluid flow through axisymmetric ducts, the time averaged governing equations, closed using the k-ε turbulence model, take the form:

continuity

$$\frac{\partial v}{\partial r}+\frac{\partial u}{\partial x}+\frac{v}{r}=0 \qquad (1)$$

u-momentum

$$u\frac{\partial \rho u}{\partial x}+v\frac{\partial \rho u}{\partial r}=\frac{\partial \sigma_{xr}}{\partial r}+\frac{\partial \sigma_{xx}}{\partial x}+\frac{\sigma_{xr}}{r} \qquad (2)$$

v-momentum

$$u\frac{\partial \rho v}{\partial x}+v\frac{\partial \rho v}{\partial r}=\frac{\partial \sigma_{rr}}{\partial r}+\frac{\partial \sigma_{xr}}{\partial x}+\frac{\sigma_{rr}-\sigma_{\theta\theta}}{r} \qquad (3)$$

w-momentum

$$u\frac{\partial \rho w}{\partial x}+v\frac{\partial \rho v}{\partial r}=\frac{\partial \sigma_{r\theta}}{\partial r}+\frac{\partial \sigma_{\theta x}}{\partial x}+\frac{2\sigma_{r\theta}}{r} \qquad (4)$$

Where the stress tensor components are given by:

$$\sigma_{xx} = -p + 2K\left(\frac{\partial u}{\partial x}\right)^n + 2\mu_t\left(\frac{\partial u}{\partial x}\right)$$

$$\sigma_{rr} = -p + 2K\left(\frac{\partial v}{\partial r}\right)^n + 2\mu_t\left(\frac{\partial v}{\partial r}\right)$$

$$\sigma_{\theta\theta} = -p + 2K\left(\frac{v}{r}\right)^n + 2\mu_t\left(\frac{v}{r}\right) \qquad (5)$$

$$\sigma_{xr} = -p + K\left(\frac{\partial v}{\partial x} + \frac{\partial u}{\partial r}\right)^n + \mu_t\left(\frac{\partial v}{\partial x} + \frac{\partial u}{\partial r}\right)$$

$$\sigma_{r\theta} = -p + K\left(\frac{\partial w}{\partial r} - \frac{w}{r}\right)^n + \mu_t\left(\frac{\partial w}{\partial r} - \frac{w}{r}\right)$$

$$\sigma_{\theta x} = -p + K\left(\frac{\partial w}{\partial x}\right)^n + \mu_t\left(\frac{\partial w}{\partial x}\right)$$

where the turbulent viscosity μ_t is obtained as $\mu_t = \frac{\rho c_\mu k^2}{\varepsilon}$. The turbulence kinetic energy (k) and its dissipation rate (ε) are obtained from their equations given as:

k-equation

$$u\frac{\partial \rho k}{\partial x} + v\frac{\partial \rho k}{\partial r} = \frac{\partial}{\partial x}\left(\frac{\mu_t}{\sigma_k}\frac{\partial k}{\partial x}\right) + \frac{1}{r}\frac{\partial}{\partial r}\left(\frac{\mu_t}{\sigma_k} r \frac{\partial k}{\partial r}\right) + G - \rho\varepsilon \qquad (6)$$

ε–equation

$$u\frac{\partial \rho \varepsilon}{\partial x} + v\frac{\partial \rho \varepsilon}{\partial r} = \frac{\partial}{\partial x}\left(\frac{\mu_t}{\sigma_\varepsilon}\frac{\partial \varepsilon}{\partial x}\right) + \frac{1}{r}\frac{\partial}{\partial r}\left(\frac{\mu_t}{\sigma_\varepsilon} r \frac{\partial \varepsilon}{\partial r}\right) + C_1 G\frac{\varepsilon}{k} - C_2 G\frac{\varepsilon^2}{k} \qquad (7)$$

Here G is the generation term, which, according to the standard k-ε model (Launder Spalding(1974)) is given by:

$$G = \mu_t\left\{2\left[\left(\frac{\partial u}{\partial x}\right)^2 + \left(\frac{\partial v}{\partial r}\right)^2 + \left(\frac{v}{r}\right)^2\right] + \left(\frac{\partial u}{\partial r} + \frac{\partial v}{\partial x}\right)^2 + \left(\frac{\partial w}{\partial r} - \frac{w}{r}\right)^2\right\} \qquad (8)$$

The values of the empirical constants used in the standard k-ε model are given below:

$$C_\mu = 0.09, C_1 = 1.44, C_2 = 1.92, \sigma_k = 1.0, \sigma_\varepsilon = 1.3$$

(Launder & Spalding (1974)).

The Turbulence model used here, was developed and usually used for Newtonian fluids. But, in the present study, the same turbulence model is used to model the turbulent part of the non-Newtonian fluid. This is used on the basis of findings by Wilson & Thomas (1985). They investigated turbulent non-Newtonian flows through pipes. The major difference compared with Newtonian fluid was found to be the thickening of viscous sub-layer. The logarithmic region of flow was found to be of similar nature. Since standard k-ε model (Launder Spalding(1974)) is used outside the viscous sublayer, it is adopted in the present study, as a reasonable option in absence of a reliable turbulece model for non- Newtonian flow.

For laminar non-Newtonian flow, the above equations are used with μ_t=0. For Newtonian fluid, the above equations are used with the exponent n=1, instead of n=0.75 used for non-Newtonian fluid.

4. THE SOLUTION PROCEDURE:

The governing equations are discretised in a finite volume fashion using a staggered arrangement of the variables. The Central difference scheme (CDS) was employed to evaluate the diffusion terms and a Hybrid scheme, made up of Upwind Difference Scheme (UDS) and CDS, was employed to evaluate the convection terms. The solutions were obtained using the SIMPLE algorithm. To obtain a solution independent of the number and spacing of the grid nodes, grid sensitivity tests were performed. It was found that the solution becomes almost grid

independent with 2600 grids in the streamwise direction and 30 grids in the cross-stream direction. Doubling the grids in both directions, produced a maximum variation of 1% in the streamwise velocity. Hence 2600x30 grid system was used in the present study.

5. RESULTS & DISCUSSION

Results obtained under laminar and turbulent conditions, for both Newtonian & Non-Newtonian fluids are presented in the form of axial and tangential velocity profiles. For turbulent flow cases, the k-ε model has been used. Figs. 2-4 show the axial velocity profiles and Figs. 5-7 show the tangential velocity profiles. In all the cases, present numerical results are compared with the experiential data of Escudier et al. (1995) at the non-dimensional axial location ξ=245. Results obtained for laminar Newtonian flow, not shown here, were found to be in exact agreement with the analytical solution at the developed stage.

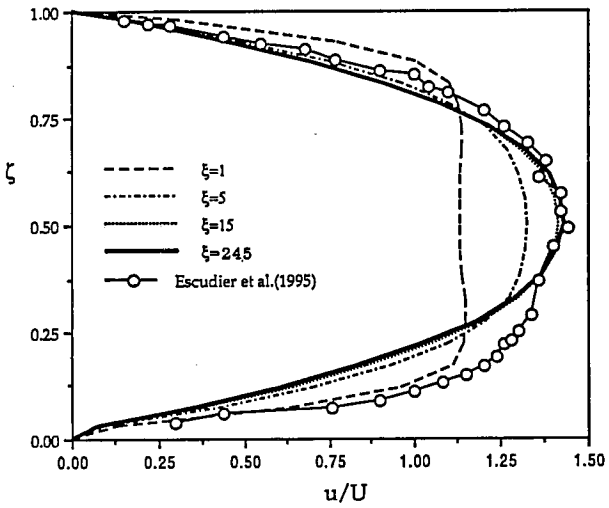

Fig.2 Axial velocity profiles for CMC (Re=350)

Fig.2. shows the gradual development of laminar non-Newtonian (CMC) axial flow at Re=350. The flow reaches its development at ξ=15. Comparisons with experimental data at ξ=245, show under prediction of velocities in the near inner-wall region. This may have been associated with the onset of turbulence due to higher rotational speed of the centerbody. Here, the Reynolds number calculated on the basis of mean axial velocity is low, but the rotational speed of the centerbody is maintained constant at a higher level, for all the Reynolds number values investigated. The experimental values of turbulent fluctuating velocities, presented in Escudier et al. (1995), also indicate the existence of substantial turbulence at Re=350. For polymeric fluids, this turbulence level is suppressed in the near inner-wall region (Escudier et al. (1995)). Suppression of turbulence results in lower shear stresses and hence higher velocities in these region. Calculations made under laminar flow assumptions are unable to reproduce this flow behavior.

Fig.3 show the gradual development of turbulence axial flow for Newtonian fluid (Glucose) at Re=7500. The predicted flow

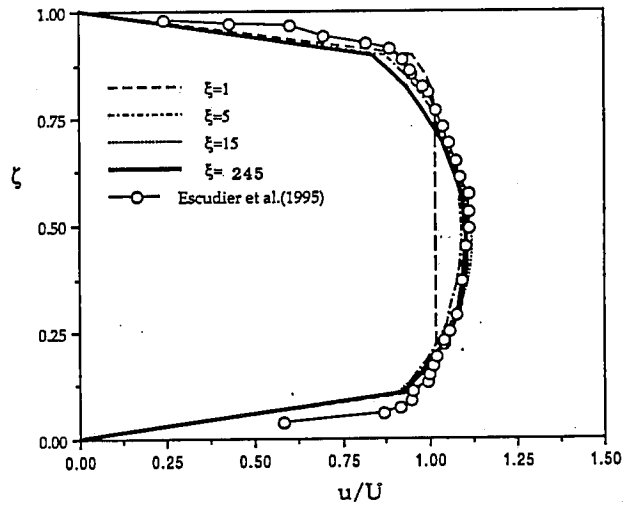

Fig.3 Axial velocity profiles for Glucose (Re=7500)

seems to attain development at ξ=15. Results compared with the experiments at ξ=245 show reasonably good agreement.

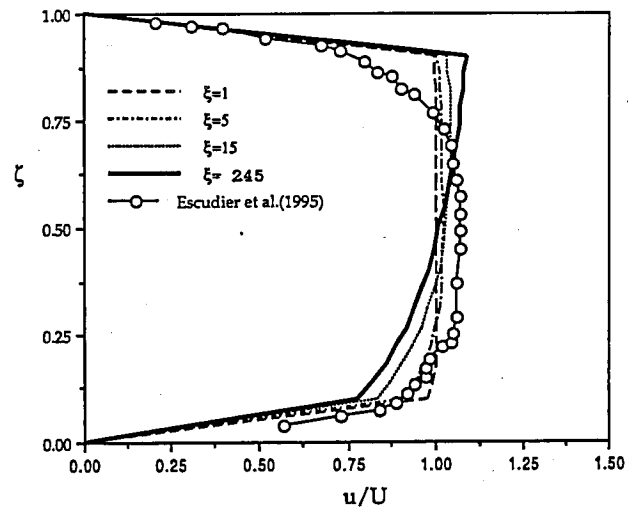

Fig.4 Axial velocity profiles for CMC (Re=4400)

The axial velocity profiles for turbulent Non-Newtonian (CMC) flow, at Re=4400, are shown in Fig.4. The flow attains development at approximately ξ=15. Results compared with the experiments at ξ=245, show under prediction in the near inner-wall region and over prediction in the near outer-wall region. This can be attributed to the deficiencies of the k-ε turbulence model used. The k-ε model is unable to reproduce the complex behavior, of suppression of turbulence, associated with the centerbody rotation. Further, the k-ε model usually over predicts the shear stresses. In the near inner-wall region, due to rotation of the centerbody, high velocity gradients are created. This leads to higher turbulent kinetic energy and hence higher shear stresses. The higher shear stresses results in lower velocities in the near inner-wall regions. The comparatively lower values of shear stresses, associated with lower values of velocity gradients in the near upper-wall region, results in higher velocities there.

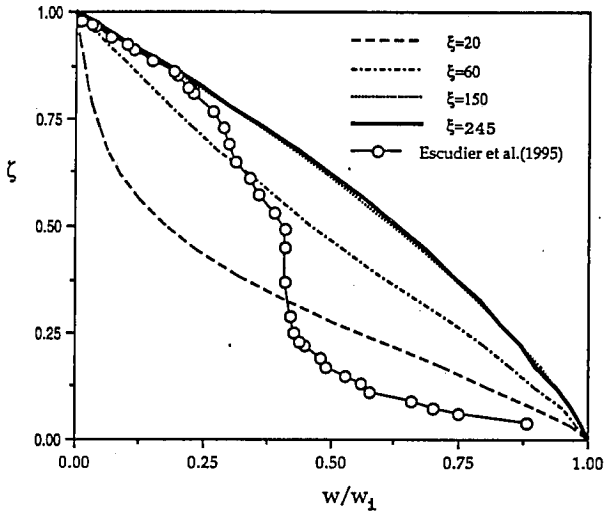

Fig.5 Tangential velocity profiles for CMC (Re=350)

Fig.5 shows the tangential velocity distributions for laminar non-Newtonian (CMC) flow at Re=350. The flow reaches its development at ξ=150. At ξ=245 the numerical results show an approximately linear variation of tangential velocity from the inner-wall to the outer-wall. Whereas, the experiments show a triple layer structure. This structure consists of: a thin layer close to the centerbody, where tangential velocity increases rapidly to match the peripheral speed of the inner-wall; a region of constant angular momentum over much of the central region of the annulus; and a thin layer in the near-outer wall region. These observations have also been made by Nouri & Whitelaw (1994) and Taylor (1935). Taylor (1935) in his study, with Newtonian fluid, argued that a dramatic change in turbulence structure occurs in the annulus leading to the triple layer structure, and the mixing length/eddy viscosity concept becomes incompatible. Escudier et al. (1995) pointed out that, the situation becomes more complex for non-Newtonian fluid. The existence of turbulence, even at Re=350 (Escudier et al. (1995)) has led to these discrepancies between prediction and experiment.

Fig.6 show the tangential velocities for Newtonian (Glucose) flow at Re=7500. Here, fully developed conditions has not been achieved, even at ξ=150. The successful reproduction of the triple layer velocity structure is evident. However, the comparisons at ξ=245, show some deviations in the central region of the annulus. This may have been due to the deficiencies of the k-ε turbulence model used. Further, the eddy viscosity concept, on which the k-ε model is developed, is incompatible with the present flow situation

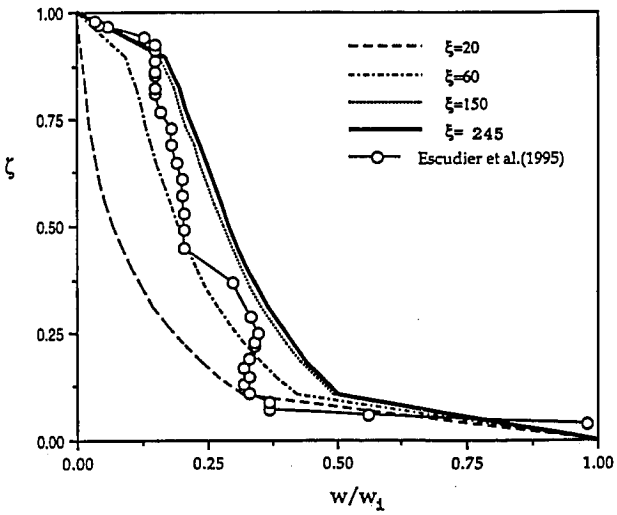

Fig.6 Tangential velocity profiles for Glucose (Re=7500)

(Taylor(1935)). The sharp changes observed in the measured (Escudier et al. (1995)) values, may have been associated with the advection of Taylor vortices in the flow. The tangential velocities for turbulent non-Newtonian (CMC) flow at Re=4400 are shown in Fig.7. The qualitative and

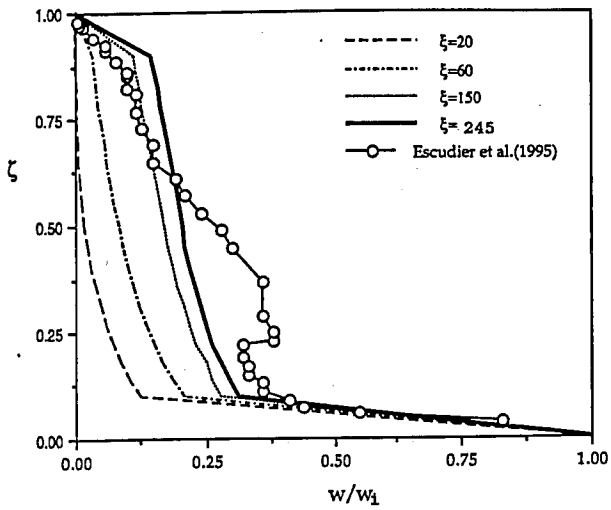

Fig.7 Tangential velocity profiles for CMC (Re=4400)

quantitative behavior of the predictions are similar to that explained for Newtonian flow.

6. CONCLUSIONS:

The laminar and turbulent flows of Newtonian and non-Newtonian fluids through a concentric annulus are investigated numerically. For laminar non-Newtonian flow, the axial velocities are under predicted and the tangential velocities are over predicted in the near inner-wall region. The major reasons for these deviations are, the presence of turbulence in the experiments and its suppression near the inner-wall. For turbulent flow, the axial velocities for Newtonian fluid are well reproduced, but the tangential velocities showed deviations. For non-Newtonian turbulent flow, both the axial and the tangential velocities showed deviations. These are attributed to the deficiencies of the eddy viscosity based turbulence model used.

REFERENCES:

Escudier, M. P. and Gouldson, 1995. "Concentric annular flow with centerbody rotation of a Newtonian and a shear-thinning liquid". Int. J. Heat and Fluid Flow, Vol. 16, No. 3, pp.156-162.

Gucuyener, H. I. and Mehmetoglu, T. 1992. "Flow of yield-pseudo-plastic fluids through a concentric annulus". AIChE Journal, Vol. 38, No. 7, pp-1139-1143.

Lockett, T. J., Richardson, S. M. and Worrakar, W. J. 1992. "The stability of inelastic non-Newtonian fluids in Couette flow between concentric cylinders: A finite element study. J. Non-Newtonian Fluid Mech., Vol. 43, pp. 165-177

Launder, B. E., and Spalding, D. B. 1974. "The numerical computation of turbulent flow", Comp. Methods Appl. Mech. Engng Vol. 3, pp. 269

Naimi, M., Deviene, R., and Lebouche, M. 1990. "Etude dynamique et thermique de lecoulement de couette-Taylor-poiseulle; cas d'un fluide presentant un seuil d'ecoulement. Int. J. Heat Mass Transfer. Vol. 33, pp. 381-391.

Nouri, J. M., and Whitelaw, J. H. 1994. "Flow of Newtonian and non-Newtonian fluids in a concentric annulus with rotation of the inner cylinder. J. Fluids Engg., Vol.116, pp. 821-827.

Sharma, B. I., Launder, B. E., and Scott, C. J. 1976. "Computation of annular, turbulent flow with rotating core fluid. J. Fluids Eng., Dec., pp. 753-758

Taylor, G.I.. 1935. "Distribution of velocity and temperature between concentric rotating cylinders". Proc. Roy. Soc. A., 494-512

Wilson, K. C., and Thomas, A. 1985, "A new analysis of the turbulent flow of Non-Newtonian Fluids". Canadian J. of Chem. Eng., Vol. 63, pp 539-546.